Environmental Health Perspectives
Vol. 60, pp. 11-28, 1985

A Mathematical Model for the Transport and Fate of Organic Chemicals in Unsaturated/ Saturated Soils

by F. Tom Lindstrom* and Warren T. Piver†

A mathematical model, simulating the transport and fate of nonionizable organic compounds in unsaturated/saturated porous media (soils) in a terrestrial microcosm has been developed. Using the principles of water mass, momentum, heat energy and chemical mass balance, the three fields: moisture, temperature, and liquid phase chemical concentration are solved for simultaneously by coupling the soil slab to an environmentally realistic air–soil interface (a dynamic free boundary) conditions and a prescribed height water table. The environmental conditions at the soil surface–air chamber interface are easily changed, via geometric scaling factors, to simulate either an open agricultural field or a landfill type of situation. Illustrative simulation runs examine the effects of different soil-chemical characteristics on hydrological and chemical concentration profiles.

Introduction

Transport and fate models for organic chemicals in soils have been in the literature for years. They are almost always, however, specific models, which have been designed to simulate the transport and fate of organic compounds in isothermal, homogeneous, water saturated, sorbing porous media. Piver and Lindstrom (*1*) and Lindstrom and Piver (*2*) have surveyed the existing literature on these models. To date, there does not appear to be any published transport and fate model for the nonisothermal, nonhomogeneous, unsaturated/ saturated sorbing porous media case except that of Lindstrom and Piver (*2*).

It is no longer adequate to ignore the influences of moisture and temperature variations (spatially and temporally) on chemical reactions and/or biological processes in soils. It is well known that microbial degradation rates are very temperature sensitive for most organic compounds. It therefore is incumbent upon the transport and fate modeler to retain as much realism, with respect to known physical and biological processes, as is possible. Just such a model, called NEWTMC, has been evolving for several years now. Presenting and demonstrating the currently available features of this model is the subject of this paper. Only the major assumptions and resulting transport equations are presented below. The reader, interested in the mathematical details of the integrated system of transport and fate equations, should consult Lindstrom and Piver (*2*). Also, the current listing of the Fortran V computer code together with an example run both on a CDC Cyber 172/720 and a DEC VAX can be found in Lindstrom and Piver (*2*).

System Assumptions and Major Features

NEWTMC is the name of the Fortran V coded algorithm for simulating the transport and fate of nonionizable organic compounds in a terrestrial microcosm (TMC). Although the model was originally designed to simulate the transport and fate of a chemical in a terrestrial microcosm whose scale is about 1 to 2 m^3 in volume (Fig. 1), the version described here is general enough to span the range of physical situations from small TMCs to large fields or landfills. The large field simulation is obtained by geometric parameter specification. Figure 2 shows a diagrammatic sketch of the CERL TMC, while Figure 3 shows a thin slab of soil in the TMC within which certain physical and biological transport and chemical conversion processes are occurring. A nomenclature list explaining all the mathematical symbols can be found in Tables 1 and 2.

*Department of Mathematics, College of Science, Oregon State University, Corvallis, OR 97331.
†National Institute of Environmental Health Sciences, P.O. Box 12233, Research Triangle Park, NC 27709.

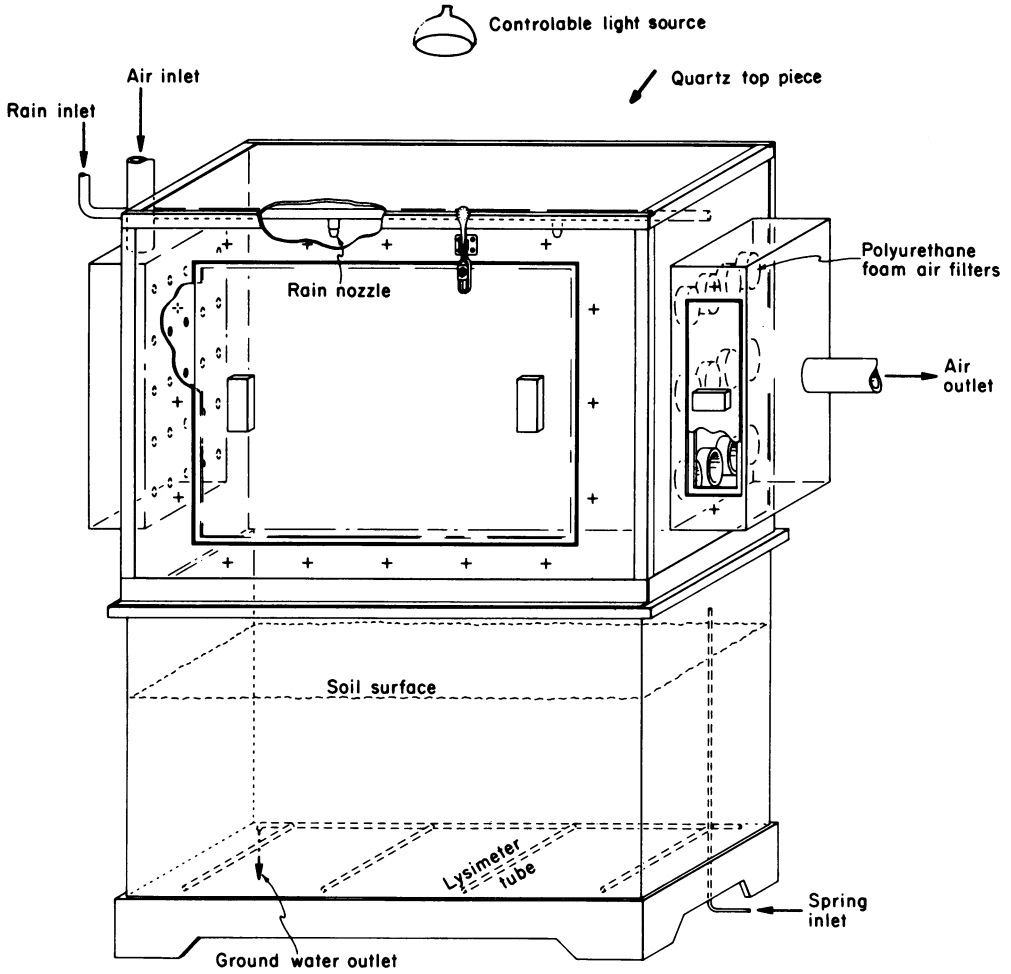

FIGURE 1. Schematic diagram of the TMC Version II.

Basic Assumptions for NEWTMC

For the air chamber, the following assumptions have been made: (1) the contents of the air chamber are instantaneously well mixed; (2) the air flow in the box is turbulent and not laminar; (3) the air inflow rate is constant in time; (4) there are no sources or sinks of air in the system anywhere; (5) the incoming air temperature and relative humidity can be characterized by Fourier series methods; (6) the light source can be readily characterized over time via off–on switch type step functions (indicator functions); (7) the chemical input and/or initial distribution is known; (8) the rain intensity and frequency are prescribed; (9) the air chamber is in intimate contact with the soil surface;

For the soil chamber the following assumptions have been made. (1) The soil can be characterized in terms of known parameters (parameteric functions of space and time possibly) such as the local bulk density ρ_b, the local porosity ϵ, the local percent, sand, clay and organic matter present, the local specific heats of the solids and water, the local heat conductivities of the soil solids and water, the local latent heat of vaporization, the local soil moisture tension function, the local soil hydraulic conductivity function and the density of water (assumed space–time and temperature independent) water vapor, and saturated water vapor in the soil voids. (2) The air chamber and soil surface are coupled together for all three fields—moisture, heat and chemical—via heat and mass transport rules operating in the top boundary layer. (3) The water table is spread uniformly over the bottom of the TMC and is assumed to be at external atmospheric conditions for water, heat, and dissolved chemical, and chemical vapor transmission at all times. (4) The initial chemical distribution in the soil is prescribed. (5) There is no flow of moisture and no flow of chemical through the lateral walls of the TMC. (6) The macroscopic transport equations are the outcomes of averaging the microscopic field equations (stochastic) over volumes of at least 1 cm^3.

Summary of Major Features of NEWTMC

In line with the above stated assumptions, NEWTMC currently has the following built-in features. (1) The model is able to predict simultaneously the moisture,

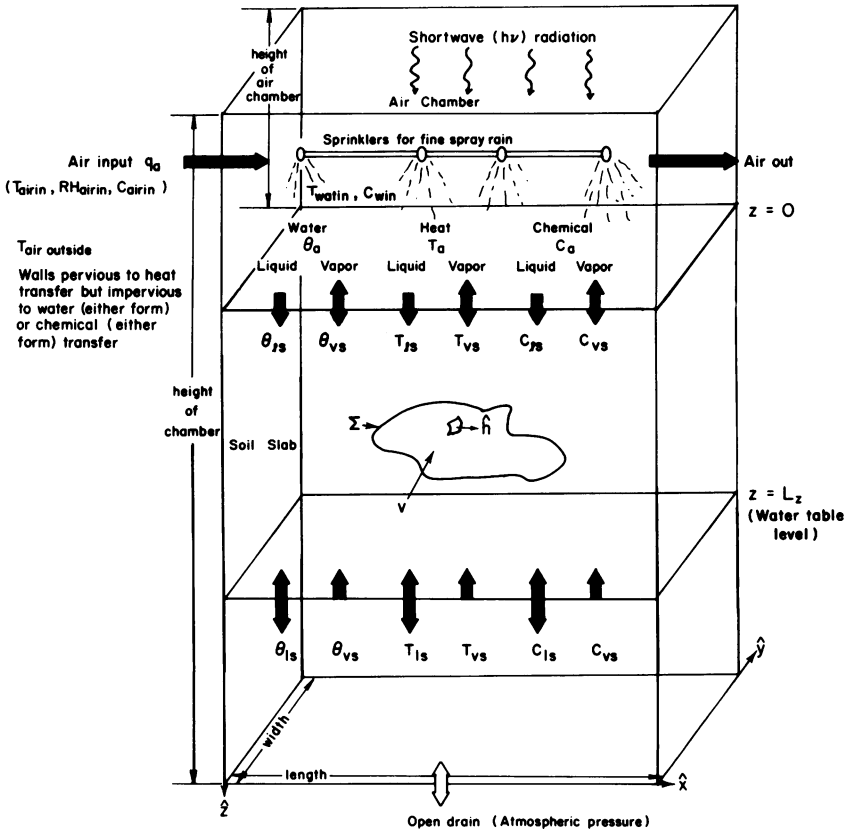

FIGURE 2. Overall design of NEWTMC.

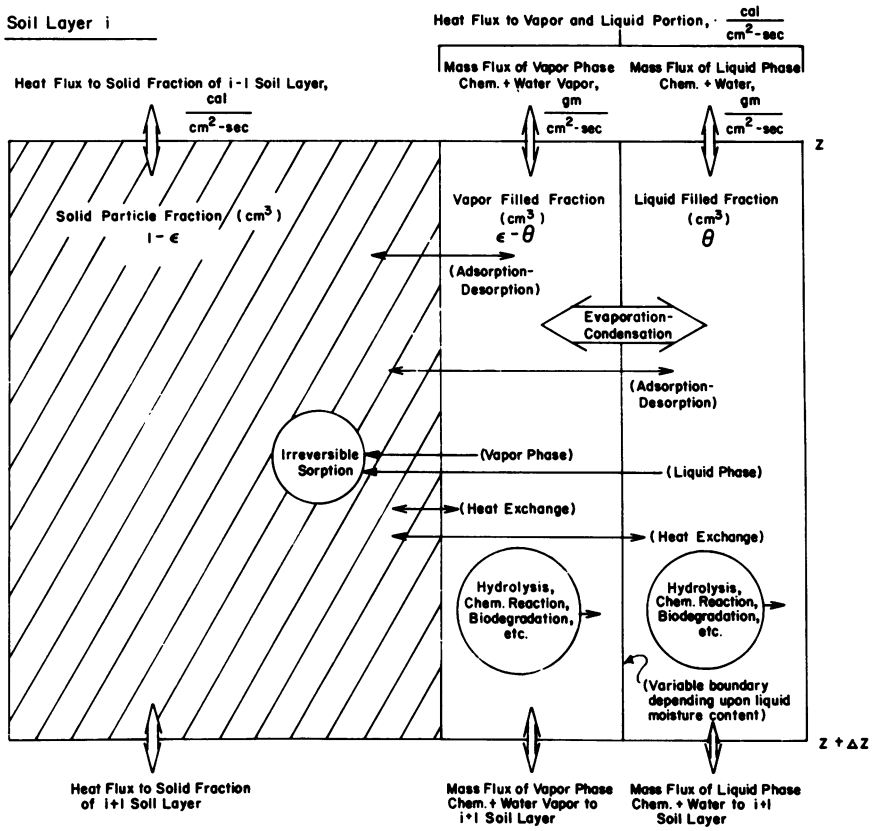

FIGURE 3. Local environment in the simple TMC in an arbitrary soil layer of thickness Δz (cm).

Table 1. Definitions of symbols and units for characterizing parameters.

Symbol	Meaning	Units
I. Soil characterizing parameters (moisture field)		
θ_s	Saturated moisture value	$= \epsilon$ (usually)
α_θ, β_θ	Parameters which with θ_s characterize moisture tension function $\psi = \psi(\theta)$	cm H_2O
α_{con}, μ_{con}, γ_{con}	Parameters which characterize the soil conductivity function $K = K(\theta)$	cm/hr
$K(\theta_s)$	Saturated soil liquid moisture conductivity	cm/hr
α_{tort}	Tortuosity factor of soil	$0 \leq \alpha_{tort} \leq 1$
ϵ	Porosity of soil	cm^3 voids/cm^3 soil
ρ_β	Bulk density of soil (formula)	g soil/cm^3 soil
$(\%)_{san}$	Decimal % sand	dimensionless
$(\%)_{org}$	Decimal % organic	dimensionless
$(\%)_{org}$	Decimal % clay	dimensionless
ρ_{sand}	Density of quartz sand	g/cm^3
$\rho_{organic}$	Density of humus	g/cm^3
ρ_{clay}	Density of illite clay	g/cm^3
ρ_{solids}	Average density of soil particles (formula)	g/cm^3
α_{soil}	Albedo of soil surface	dimensionless
α_{water}	Albedo of water surface	dimensionless
α_{air}	Albedo of water vapor saturated air	dimensionless
λ_{air}	Conductivity of air at 20°C	cal/cm-hr-°K
λ_{water}	Conductivity of water at 20°C	cal/cm-hr-°K
λ_{sand}	Conductivity of sand particles	cal/cm-hr-°K
$\lambda_{organic}$	Conductivity of organic particles	cal/cm-hr-°K
λ_{clay}	Conductivity of clay	cal/cm-hr-°K
λ_{solids}	Average conductivity of solids (formula)	cal/cm-hr-°K
c_{air}	Specific heat of air (moist)	cal/g-°K
c_w	Specific heat of water	cal/g-°K
c_{sand}	Specific heat of sand (quartz)	cal/g-°K
c_{org}	Specific heat of humus	cal/g-°K
c_{clay}	Specific heat of illite clay	cal/g-°K
c_{solids}	Average specific heat of solids (formula)	cal/g-°K
ϵH_2O	Emissivity of water	dimensionless
ϵ_{plexi}	Emissivity of the Plexiglass wall of the TMC	dimensionless
ϵ_{air}	Emissivity of the air above the soil surface	dimensionless
ϵ_{soil}	Emissivity of soil	dimensionless
H_c	Henry law constant	dimensionless
$D_{l\phi}$	Liquid-phase molecular diffusion coefficient	cm^2/hr
$D_{V\Phi}$	Vapor-phase molecular diffusion coefficient	cm^2/hr
α_{disp}	Chemical hydrodynamic dispersion velocity constant	cm
K_{dl}	Liquid-phase reversible linear sorption rule constant (formula)	cm^3soil water/cm^3soil
K_{dv}	Vapor-phase reversible linear sorption (formula)	cm^3soil water vapor cm^3soil
γ_l	Liquid-phase irreversible first-order sorption constant	hr^{-1}
γ_v	Vapor-phase irreversible first-order sorption constant	hr^{-1}
α_l	Liquid-phase hydrolysis rate constant	hr^{-1}
α_v	Vapor-phase hydrolysis rate constant	hr^{-1}
β_l	Liquid-phase biodegradation rate constant	hr^{-1}
β_v	Vapor-phase biodegradation rate constant	hr^{-1}
α_a	Air chamber hydrolysis rate coefficient	hr^{-1}
K_{vap}	Vaporization rate constant air soil-air chamber interface	μg/hr
II. Moisture and hat field vapor parameters for soil and air chamber		
D_{atm}	Water vapor molecular diffusion	$\equiv 0.265$ cm^2/sec
P_{ress}	Air pressure in air chamber and soil	mm Hg
ρ_{air}	Density of air	0.0011 g/cm^3
ρ_w	Density of liquid water	1.0 g/cm^3
β_{Tvap}	Temperature effect saturated water vapor density constant	cm/cm^3-°K
E_{con}	Vaporization of water constant (overall)	cm/hr
β_{vap}	Vaporization of water due to wind speed constant	hr/cm
WS	Wind speed	cm/hr
γ_{Tliq}	Moisture tension temperature effect parameter	$°K^{-1}$
£	Latent heat of evaporization	cal/g
β_{TMC}	Wall reflection factor for TMC interior walls	dimensionless
D_H	Sensible heat transfer parameter	cm/hr
κ_{plexi}	Thermal conductivity of TMC Plexiglass wall	cal/cm-hr-°K
$UV_r(t)$	Ultraviolet light chemical decomposition function (photolysis constant)	1/mm Hg-hr
T_{air}	Temperature of air outside of the TMC	°K
$q_{swr}(t)$	Shortwave radiation flux density	cal/cm^2-hr
H_{plexi}	Average area Plexiglass wall heat	cal/cm^2-hr-°K

Table 1. (continued)

Symbol	Meaning	Units
III. Geometrical parameters		
V_a	Volume of air chamber	cm^3
A	Surface area of air chamber–soil surface interface	cm^2
A_{wall}	Total inside surface area of air chamber minus soil surface area	cm^2
q_a	Volumetric air flow rate in air chamber	cm^3/hr
V_l	Volume of ith soil layer	cm^3
Δz_i	Thickness of ith soil layer	cm
δ_{plexi}	Thickness of TMC Plexiglass wall	cm
IV. Miscellaneous single constants		
g	Gravitational constant	1.27×10^{10} cm/hr^2
R	Gas constant	5.98×10^{13} cm^2/hr^2-°K
σ	Stefan-Boltzmann constant	4.90×10^{-9} cal/hr-cm^2-°K^4
π	3.1416	radians

Table 2. Definition of symbols and units for system variables.

Symbol	Meaning	Units
I. Air chamber		
C_a	Air chamber chemical concentration	g/L air
T_a	Temperature in air chamber	°K
θ_a	Relative humidity in air chamber	dimensionless
X_{ca}	Mass of chemical in air chamber	μg
X_{ha}	Heat content of air chamber	cal
X_{ma}	Mass of water in air chamber	g
II. Soil (general)		
$C_{l,z,t}$	Soil–water liquid-phase chemical concentration	μg/cm^3 H_2O
C_M (z,t)	Soil vapor phase chemical concentration	μg/cm^3 air
T (z,t)	Soil temperature field	°K
Θ (x,t)	Soil-water content	cm^3 water/cm^3 soil
X_l	Soil-bound chemical mass (liquid phase)	μg
X_v	Soil-bound chemical mass (vapor phase)	μg
III. Soil layer i		
C_i (t)	Soil-water liquid-phase chemical concentration at geometric center of soil layer i	μg/cm^3 H_2O
C_i*(t)	Soil-water liquid-phase chemical concentration on the boundary between layers i and $i + 1$	μg/cm^3 H_2O
T_i (t)	Temperature distribution in soil at the geometric center of soil layer i	°K
T_i*(t)	Temperature distribution in soil on the boundary between layers i and $i + 1$	°K
θ (t)	Soil moisture content at the geometric of soil layer i	cm^3 water/cm^3 soil
θ_i (t)	Soil moisture content on the boundary between layers i and $i + 1$	cm^3 water/cm^3 soil
X_{ci}	Total mass of chemical in soil layer i	μg
X_{hi}	Total heat content in soil layer i	cal
X_{mi}	Total moisture content in soil layer i	g water
IV. Soil–air chamber interface		
T_{watin} (t)	Temperature of incoming rainwater	°K
$C_{wat\ in}$ (t)	Chemical concentration in incoming rain water	μg/cm^3
Q_{rain} (t)	Volume flow rate of incoming rainwater	cm^3/hr
V. Soil–water table interface		
T_{gndwat} (t)	Temperature of groundwater	°K
C_{gndwat} (t)	Chemical concentration in groundwater	μg/cm^3
VI. Air chamber (air input port)		
$T_{air\ in}$ (t)	Temperature of incoming air	°K
$RH_{air\ in}$ (t)	Relative humidity of incoming air	dimensionless
$C_{air\ in}$	Chemical concentration in incoming air	μg/cm^3 air
VIII. Soil slab		
$V_l(z,t)$	Instantaneous liquid water velocity field vector	cm/hr
V_v (z,t)	Instantaneous water vapor velocity field vector	cm/hr
n, or z	Instantaneous unit normal vector to plane dimensionless $z = 0$ with positive orientation vertically downward	

heat and chemical fields in both the air chamber over the soil slab and the soil slab itself. (2) The model simulates an open field situation or those conditions over a landfill by setting the height of the air chamber to a very large value as well as setting q_a, the volumetric air flow rate through the air chamber, simultaneously large so WS, the wind speed, remains fixed at the desired value. (3) The timing and intensity of both light and rain events can be very freely specified a priori. (4) A great many different atmospheric conditions (high-low humidity, high-low temperature, high-low wind speed) can be represented with ease. (5) Chemical, water and heat are all balanced and accounted for at all points in time and space with this balance information printed out at user specified times. (6) The free air–soil surface boundary is modeled dynamically so as to allow field variables to seek their appropriate values (they are not rigidly fixed or otherwise specified over time).

(7) Chemical may be administered via: incoming air (vapor phase), rain water, flow in from the water table or initially distributed in the soil slab. (8) The soil slab need not be spatially homogeneous but may in fact grade from one soil type to another with the latitude of soil properties being input information.

System Equations

In the air chamber the moisture balance equation is given by Eq. (1):

$$dX_{ma}/dt = Q_{mwaain} - Q_{mwaaot} + Q_{evap_l} + Q_{vap} \quad (1)$$

where dX_{ma}/dt is the instantaneous rate of change of water mass in air chamber per hour (g/hr).

Q_{mwaain}, the mass of water input via incoming air per hour (g/hr) is given as:

$$Q_{mwaain} = q_a \rho_{wv}^{sat}[(T_{air\ in}(t)]\mathrm{RH}_{air\ in}(t) \quad (2)$$

Q_{mwaaot}, the mass of water lost via air per hour (g/hr) is given by

$$Q_{mwaaot} = q_a \theta_a \rho_{wv}^{sat}(T_a) \quad (3)$$

Q_{evap_l}, the evaporation of water from soil system (g/hr)

$$Q_{evap_l} = AE_{con}\theta_o^*(1 + \beta_{vap}\mathrm{WS})[\rho_{wv}^{sat}(T_o^*)h - \rho_{wv}^{sat}(T_a)\theta_a] \quad (4)$$

Q_{vap}, the diffusion of water vapor from the soil surface is given by

$$Q_{vap} = \mathrm{A}(\epsilon_o - \theta_o^*)D_{atm}\alpha_{tort}\left.\frac{\partial \rho_{wv}}{\partial z}\right|_{z=0} \quad (5)$$

and

$$Q_{evap} = Q_{vap_l} + Q_{evap} \quad (6)$$

with

$$E_{con} = 0.001\rho_w/\rho_{air} \quad (7)$$

The relative humidity expression

$$h = \rho_{wv}(T)/\rho_{wv}^{sat}(T) = \exp\{\psi g/RT\} \quad (8)$$

comes from Edlefson and Anderson (*3*). We represent the saturated water vapor density via a low-order spline function, with the parameters obtained, via least-square regression, over the range 0°C–50°C (*4*).

The heat balance for the air chamber is given by Eq. (9):

$$dX_{ha}/dt = Q_{heatin} - Q_{heatot} + Q_{htevp} + Q_{htlwrs} - Q_{htlwra} + Q_{htssl} + Q_{htswr} - Q_{htwalls} \quad (9)$$

where dX_{ha}/dt is the instantaneous rate of change of heat in air chamber per hour (cal/hr), Q_{heatin} is the heat input via incoming moist air (cal/hr), Q_{heatot} is the heat output via exiting moist air (cal/hr), Q_{htevp} is the heat input via evaporation of water from the transfer of latent heat from soil surfaces (cal/hr), Q_{htlwrs} is the heat input via long wave radiation from the top of the soil slab (cal/hr), Q_{htlwra} is the heat output via long wave radiation to the top of the soil slab (cal/hr), Q_{htssl} is the heat input via transfer of sensible heat to air from top of soil (a signed quantity) (cal/hr), Q_{htswr} is the heat input via reflection of shortwave radiation off the top of soil slab (cal/hr) and $Q_{htwalls}$ is the heat output or input via conduction through the air chamber walls (a signed quantity) (cal/hr). The various heat flow functions in Eq. (9) are defined analogously to those of the moisture field introduced in Eq. (1). The complete set of definitions of all heat flow functions can be found in Lindstrom and Piver (*2*).

The chemical balance equation in the air chamber is given by:

$$dX_{ca}/dt = Q_{mchain} - Q_{mchaot} + Q_{mcv1s} + Q_{mcv2s} + P_{lach} - P_{lacp} \quad (10)$$

where dX_{ca}/dt is the instantaneous rate of change of chemical mass (vapor phase) (μg) per unit time (hour), Q_{mchain} is the chemical vapor mass input via incoming air (μg/hr), Q_{mchaot} is the chemical vapor output via exiting air (μg/hr), Q_{mcv1s} is the chemical input via volatilization from liquid phase from the top of the soil slab (μg/hr), Q_{mcv2s} is the chemical input via vapor-phase chemical transports out of the top of the soil slab (μg/hr) (signed quantity), P_{lach} is the chemical lost via hydrolysis processes in air chamber (μg/hr) and P_{lacp} is the chemical lost via photolysis processes in the air chamber (μg). Again, the chemical vapor mass flows, have been completely defined in Lindstrom and Piver (*2*).

Air Chamber Relative Fields

The air chamber moisture content (relative humidity) is defined via the equation:

$$\theta_a = X_{ma}/[V_a \rho_{wv}^{sat}(T_a)] \quad \text{(dimensionless)} \quad (11)$$

while the temperature field (°K) in the air chamber is defined by the expression:

$$T_a = X_{ha}/(V_a \rho_{air} c_{air}) \quad (12)$$

and the chemical concentration in the air chamber (g/cm^3 air) is defined via the rule:

$$C_a = X_{ca}/V_a \quad (13)$$

Soil Slab Field Equations

In NEWTMC we assume there are no sources or sinks of water within the soil chamber and that elemental soil volumes and surfaces are neither deforming nor translating in space or time. All sources and sinks of moisture occur in the boundary conditions and the arbitrary elemental volume v is time-independent (Fig. 2).

Using the balances of water mass and momentum in v we are ultimately lead to the conservation equation:

$$\int_v \frac{\partial[\rho_w\theta + \rho_{wv}^{sat}(T)h(\epsilon - \theta)]dv}{\partial t} = -\int_\Sigma \vec{q}_T \cdot \hat{n} ds \quad (14)$$

where

$$\vec{q}_T = \vec{q}_l + \vec{q}_v \quad (15)$$

with

$$\vec{q}_l = \theta\rho_w \left[-\underset{\leftrightarrow}{D}_{\theta l} \cdot \nabla\theta - \underset{\leftrightarrow}{D}_{Tl} \cdot \nabla T + \underset{\leftrightarrow}{K}^* \cdot \hat{z}\left(1 - \frac{\partial\psi}{\partial z}\right)\right] \quad (16)$$

and:

$$\vec{q}_v = (\epsilon - \theta)\rho_{wv}\left(-\underset{\leftrightarrow}{D}_{\theta v} \cdot \nabla\theta - \underset{\leftrightarrow}{D}_{Tv} \cdot \nabla T - \underset{\leftrightarrow}{D}_{\psi z}\frac{\partial\psi}{\partial z} \cdot \hat{z}\right) \quad (17)$$

The six indicated second-rank tensor field functions have been defined in Lindstrom and Piver (*2*).

Heat Field Equations

By defining the heat balance equation (integral form) in analogy with the moisture balance equation we arrive at the form:

$$\int_v \frac{\partial}{\partial t}\{[(1-\epsilon)c_{solids}\rho_{solids} + c_{air}(\epsilon - \theta)\rho_{air} + c_w\theta\rho_w]T\}dv = \int_\Sigma -\vec{H}\cdot\hat{n}ds \quad (18)$$

where

$$\vec{H}_S = (1 - \epsilon)\vec{H}_{ss} + \theta\vec{H}_{sl} + (\epsilon - \theta)\vec{H}_{sv} \quad (19)$$

with the individual components defined as:

$$\vec{H}_{ss} = -\underset{\leftrightarrow}{\lambda}_{solids}(z) \cdot \nabla T \quad (20)$$

$$\vec{H}_{sl} = -\lambda_w \nabla T + c_w\rho_w\vec{V}_l T \quad (21)$$

$$\vec{H}_{sv} = -\pounds(T)D_{atm}\alpha_{tort}\nabla\rho_{wv} - \lambda_{air}\nabla T \quad (22)$$

Lindstrom and Piver (*2*) discuss the representations for the latent heat function, $\pounds(T)$, and the average soil solids heat conductivity function, $\lambda_{solids}(z)$, as well as the functions, $c_{solids}(z)$, and $\rho_{solids}(z)$.

Chemical Field Equations

The total chemical flux (g chemical/cm^2-hr) through an incremental portion of the surface Σ can be written as:

$$\vec{q}_{cT} = \theta\vec{q}_{cl} + (\epsilon - \theta)\vec{q}_{cv} \quad (23)$$

where the flow path averaged liquid phase chemical flux is:

$$\vec{q}_{cl} = -\underset{\leftrightarrow}{D}_{cl} \cdot \nabla C_l + \vec{V}_l C_l \quad (24)$$

and the flow path averaged vapor phase chemical flux is represented by the expression:

$$\vec{q}_{cv} = -\underset{\leftrightarrow}{D}_{cv} \cdot \nabla C_l \quad (25)$$

Assuming linear sorption and/or rapid equilibrium partitioning of the organic compound into the organic portions of the soil (e.g., dissolution into humus), a simple Henry's law partition between the chemical in the liquid phase and the vapor phase, and three types of first-order loss processes such as biodegradation, hydrolysis and irreversible sorption and/or first-order

chemical reaction leads to the chemical mass conservation equation:

$$\int_v \frac{\partial}{\partial t}(1 + \rho_B K_{dl})[1 + (\epsilon - \theta)(1 + \rho_B K_{dv})H_c]C_l dv = \int_\Sigma - \vec{q}_{CT} \cdot \hat{n} ds - \int_v [(\% \text{ organic}) \beta_l + \gamma_l]\theta C_l dv - \int_v [\alpha_l \rho_w + \alpha_v(\epsilon - \theta)H_c \rho_{wv}^{sat}(T)h]C_l dv \quad (26)$$

We remind the reader that the coefficients β_l, γ_l, α_l and α_v are all usually strongly temperature-dependent. It is very easy to incorporate this temperature dependence in NEWTMC for the three process laws for loss of chemical (structural decomposition or irreversible sorption) from each infinitesimal volume element because they are defined in subroutine FLOWS and Fortran code changes are easily made.

Boundary and Initial Conditions

Before we can solve the system of six coupled nonlinear equations [(1), (9), (10), (14), (18) and (26)], we must adjoin initial and boundary data (conditions). The initial conditions are user specified, such as, how the moisture, heat and chemical are initially distributed in the TMC. The boundary conditions are much more complicated and will not be stated here. Lindstrom and Piver (*2*) give a detailed discussion of the boundary conditions currently built into NEWTMC. It suffices to say that the "free boundary" which exists at the air chamber-soil slab interface is very complex and must be handled with care. This has been done in NEWTMC.

Discrete System Approximations

The usual ways of approximately solving these nonlinear parabolic equations are those of finite differences (*5–7*) or finite elements (*8–13*). In either case we trade off the continuous system. This discrete approximation is formally analogous to a compartment or conceptualized system. For the remainder of this work we make the following additional assumptions: (1) the mass and heat transport phenomena in the soil are one-dimensional only, vertically, with the positive orientation being downward; and (2) the soil "slab" is partitioned into a finite number of adjoining soil layers (NSLYRS) with each layer being specified by its characteristic thickness Δz_i and its induced volume V_i. Note that $V_i = A\Delta z_i$.

Figure 4 illustrates the partitioning of the soil "column" or "slab" together with the major mass and

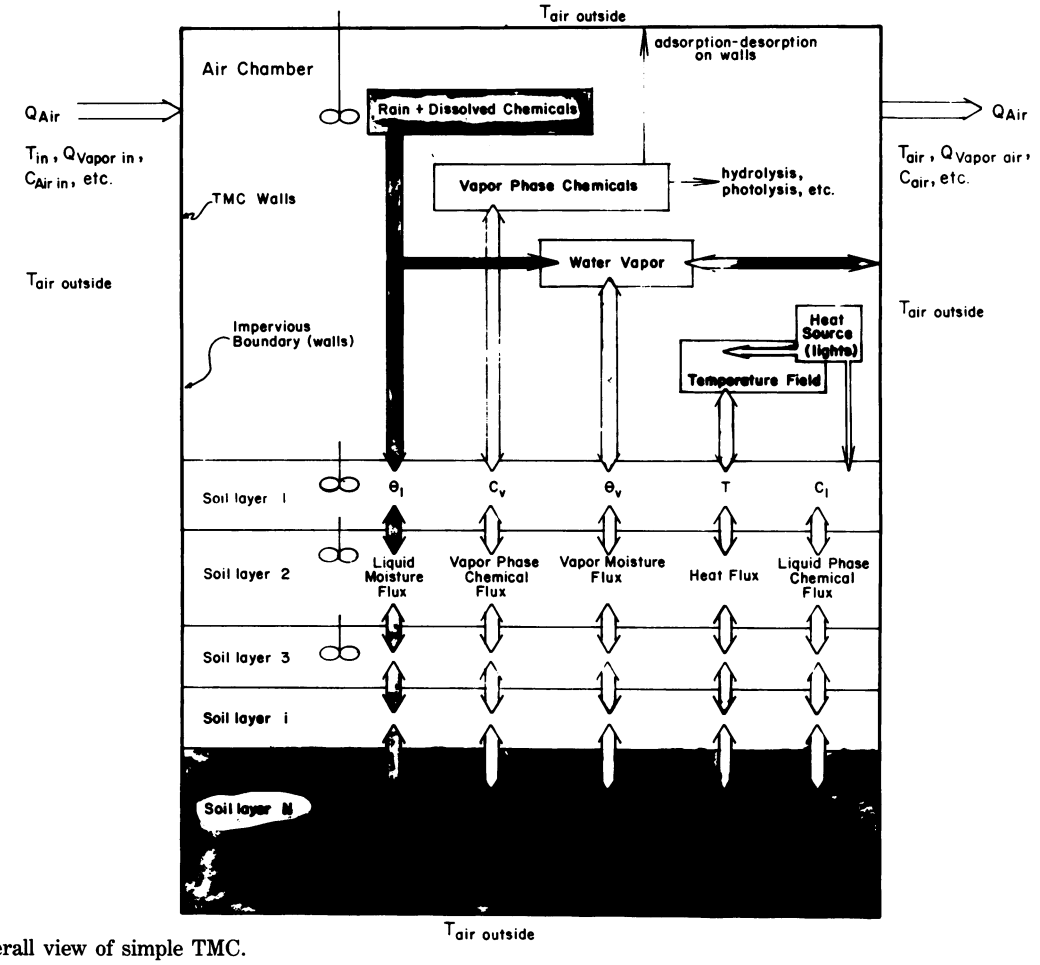

FIGURE 4. Overall view of simple TMC.

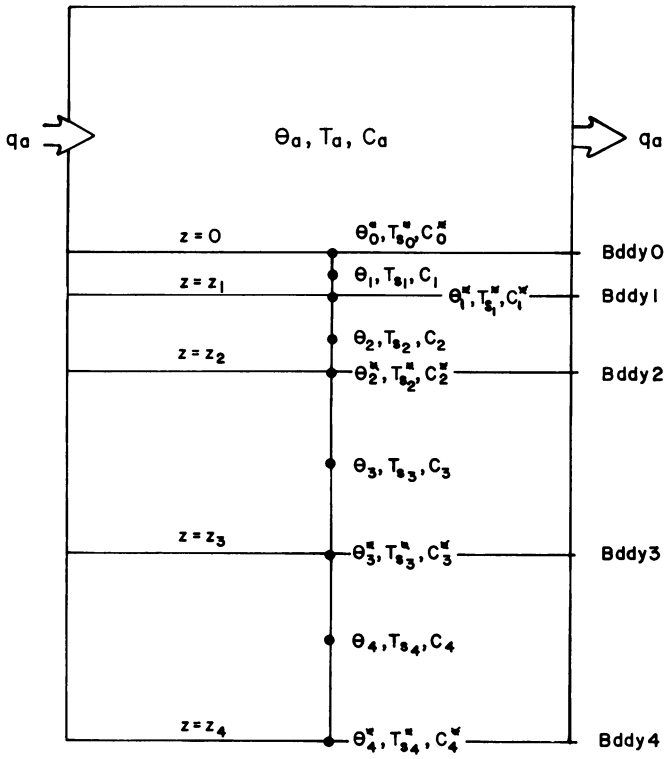

FIGURE 5. An example of the partitioning of the soil into four layers with the placement of nodal points as shown. For fluxes, starred variables are used and for processes, unstarred variables are used.

heat transport pathways in the TMC. Figure 5 illustrates an example of the placement (in space) of the assumed average and interpolating field values.

Moisture Field in the Soil Slab

Beginning with Eq. (13) the assumption of an average mass of water all concentrated at the geometric center of the kth slab (layer) of soil bounded by planes z_{k-1} and z_k is now made so that we have the ordinary differential equation approximation for layer k given as:

$$\left.\frac{dX_{\mathrm{Mk}}}{dt}\right|_{z_{k-1/2}} = +A[q_{T_z}(z_{k-1}) - q_{T_z}(z_k)] \tag{27}$$

where

$$z_{k-1} + \Delta z_k \qquad k = 1, 2,.., \mathrm{NSLYRS}$$

$$z_0 = 0$$

Interestingly enough, had we started with the conceptual approach we would have arrived at exactly this same ordinary differential equation. q_{T_z} is now substituted into Eq. (27) with due regard to the fact that only part of the surfaces at z_{k-1} and z_k contribute to the flow of moisture in each of the two respective phases. When this substitution is made, the equation is:

$$\left.\frac{dX_{\mathrm{Mk}}}{dt}\right|_{z_{k-1}} = A\left\{[\rho_w\theta V_{lz} + \rho_{wv}(\epsilon - \theta)V_{vz}]\Big|_{z_{k-1}} \times [\rho_w\theta V_{lz} + \rho_{wv}(\epsilon - \theta)V_{vz}]\Big|_{z_k}\right\} \tag{28}$$

as the final form of the moisture flow equation for layer k, where:

$$\rho_w V_{lz} = -\rho_w D_{\theta l}\frac{\partial\theta}{\partial z} - \rho_w D_{Tl}\frac{\partial T}{\partial z} + \rho_w K(\theta)\left[1 - \frac{\partial\psi}{\partial z}\right] \tag{29}$$

$$\rho_{wv}V_{vz} = -\rho_{wv}D_{\theta v}\frac{\partial\theta}{\partial z}\rho_{wv}D_{Tv}\frac{\partial T}{\partial z} - \rho_{wv}D_z\frac{\partial\psi}{\partial z} \tag{30}$$

Implicit in Eq. (27) is the definition of the time rate of change of total water in the kth layer which is given as:

$$X_{\mathrm{Mk}} = A\Delta z_k\rho_w\theta(z_{k-1/2}) + \rho_{wv}^{\mathrm{sat}}[T(z_{k-1/2})]h[\epsilon - \theta(z_{k-1/2})](\mathrm{gH_2O}) \tag{31}$$

However, since $h \cong 1.0$ for $0.10 \leqslant \theta \leqslant \theta_s$ for most soils (*14*), and ρ_{wv}^{sat} is three to four orders of magnitude less than ρ_w for most field situations (clearly controllable in the TMC), the second term in Eq. (31) is neglected, leaving the reasonable approximation for total water in the kth layer as:

$$X_{\mathrm{M}k} \doteq A\Delta z_k\rho_w\theta(z_{k-1/2}) \tag{32}$$

from which we readily obtain:

$$\theta(z_{k+1/2}) \doteq X_k/V_k\rho_w \tag{33}$$

Equation (27) is a mass balance equation for water. The instantaneous time rate of change of water in the kth soil layer is equal to the difference between the inflow (or outflow) of moisture from the k–1 layer and the outflow (or inflow) of moisture from the k layer to the k + 1 layer. Since the quantities $\rho_w V_{l_z}$ and $\rho_{wv}V_{v_z}$ are components of the total moisture flux vector they can represent either positive (downward transport) or negative (upward transport) flow of moisture across any and all of the artificially introduced boundaries (soil layer interfaces). Thus, for example, the flow of moisture from the bottom of soil layer k–1 becomes the source of moisture into the top of layer k, and so forth, for the other layers. At each soil layer interface the

principles of continuity of flux in the normal component of moisture flow and continuity in moisture tension (pressure field) are applicable.

Heat Field in the Soil Slab

Proceeding exactly as before in the moisture field case, we consider the flow of heat into and out of the two bounding planes z_{k-1} and z_k (one-dimensional heat transport assumed), and the total heat content of soil layer k is placed at the geometric center of the layer. This heat content is given the interpretation of being an average heat value for the kth layer. The space integrals indicated in Eq. (18) become:

$$\left.\frac{dX_{\mathrm{H}k}}{dt}\right|_{z_{k-1/2}} = A[\theta H_s(z_{k-1}) - (\epsilon - \theta)H_s(z_k)] \quad (34)$$

With due regard to the three different portions of the soil layer, Eq. (33) can be written as:

$$\begin{aligned}\left.\frac{dX_{\mathrm{H}k}}{dt}\right|_{z_{k-1/2}} &= A\left[-(1-\epsilon)\lambda_{\mathrm{sol}}\frac{\partial T}{\partial z} - \lambda_{\mathrm{air}}\theta\frac{\partial T}{\partial z}\right. \\ &\quad - (\epsilon-\theta)\left(\pounds D_{\mathrm{atm}}\alpha_{\mathrm{tort}}\frac{\partial \rho_{\mathrm{wv}}}{\partial z} + \lambda_{\mathrm{air}}\frac{\partial T}{\partial z}\right. \\ &\quad \left.\left. + \rho_{\mathrm{w}}\theta c_{\mathrm{w}}V_{l_z}T\right]\right|_{z_{k-1/2}} - A\left[-(1-\epsilon)\lambda_{\mathrm{sol}}\frac{\partial T}{\partial z}\right. \\ &\quad \left.\left. - (\epsilon-\theta)\left(\pounds D_{\mathrm{atm}}\alpha_{\mathrm{tort}}\frac{\partial \rho_{\mathrm{wv}}}{\partial z} + \lambda_{\mathrm{air}}\frac{\partial T}{\partial z}\right) + \rho_{\mathrm{w}}\theta c_{\mathrm{w}}V_{l_z}T\right]\right|_{z_k} \end{aligned} \quad (35)$$

We give Eq. (35) the equivalent heat balance interpretation as we gave mass balance interpretation to Eq. (28). That is, the instantaneous time rate of change of heat in the kth soil slab is equal to the difference between the inflow (outflow) of total heat (conduction + convection + latent heat) from (to) soil layer z_{k-1} and the outflow (inflow) of total heat to (from) soil layer z_{k+1}.

The heat field (average) and the temperature field in layer k are related via the expression:

$$\begin{aligned}X_{hk} = V_k[&(1-\epsilon_k)c_{\mathrm{solids}k}\rho_{\mathrm{solids}k} + (\epsilon_k - \theta_k)c_{\mathrm{air}}\rho_{\mathrm{air}} \\ &+ c_{\mathrm{w}}\theta_k\rho_{\mathrm{w}}]T_k(\mathrm{cal})\end{aligned} \quad (36)$$

from which we find the average temperature field value in the kth soil layer is:

$$T(z_{k-1/2}) = \frac{X_{\mathrm{H}k}}{V_k[(1-\epsilon_k)c_{\mathrm{solids}k}\rho_{\mathrm{solids}k} + (\epsilon_k - \theta_k)c_{\mathrm{air}}\rho_{\mathrm{air}} + c_{\mathrm{w}}\theta_k\rho_{\mathrm{w}}]} \quad (37)$$

Proceeding as in the moisture and heat flow cases, we consider chemical flow to be only one dimensional in space and the integrals to represent total values which may be replaced by average chemical mass values placed at the geometric center of the soil layer bounded by the planes z_{k-1} and z_k.

Chemical Field in the Soil Slab

Carrying this out yields, based upon Eq. (26):

$$\begin{aligned}\left.\frac{dX_{ck}}{dt}\right|_{zk-1/2} &= A[\theta q_{Clz} + (\epsilon - \theta)q_{Cvz}]\Big|_{z_{k-1}} \\ &\quad - A[\theta q_{Clz} + (\epsilon - \theta)q_{Cvz}z_k - \Lambda(\theta)C_{lk}\end{aligned} \quad (38)$$

where

$$q_{Clz} = -D_{Clz}\frac{\partial C_l}{\partial z} + V_{vz}C_l \quad (39)$$

$$q_{Cvz} = -D_{C_{\mathrm{v}}}H_c\frac{\partial C_l}{\partial z} \quad (40)$$

and

$$\begin{aligned}\Lambda(\theta) = V_k[&\beta_l\theta(\%_{\mathrm{org}}) + \beta_{\mathrm{v}}(\epsilon - \theta)(\%_{\mathrm{org}}) \\ &+ \gamma_l\theta + \alpha_l\rho_{\mathrm{w}}\theta + \alpha_{\mathrm{v}}(\epsilon - \theta)H_c\rho_{\mathrm{wv}}^{\mathrm{sat}}h]\end{aligned} \quad (41)$$

The average absolute chemical mass in soil layer k, X_{C_k}, and the average liquid phase chemical concentration, C_k, in soil layer k are related via the expression:

$$\begin{aligned}X_{Ck} = V_k[&\theta_k(1 + \rho_{\mathrm{B}k}K_{\mathrm{dl}k}) \\ &+ (\epsilon_k - \theta_k)(1 + \rho_{\mathrm{B}k}K_{\mathrm{dv}k})H_c]C_{lk}\end{aligned} \quad (42)$$

Solving for C_{lk} in terms of X_{C_k} yields for the average chemical concentration (g chemical/cm^3 water) in the liquid phase in soil layer k:

$$C_{lk} = \frac{X_{Ck}}{V_k[\theta_k(1 + \rho_{\mathrm{B}k}K_{\mathrm{dl}k}) + (\epsilon_k - \theta_k)(1 + \rho_{\mathrm{B}k}K_{\mathrm{dv}k})H_c]} \quad (43)$$

Simulations of Moisture and Chemical Transport in Unsaturated Soils

To examine representative responses in an unsaturated soil, four simulation runs were made. Detailed documentations describing the computer code are available in Lindstrom and Piver (*2*). The program is of modular design using a main program to call different subroutines in a prescribed sequence with COMMON statements used to link the different subroutines. The sequence and order of call are shown in Figure 6. Because of the simplifications of the model, the storage

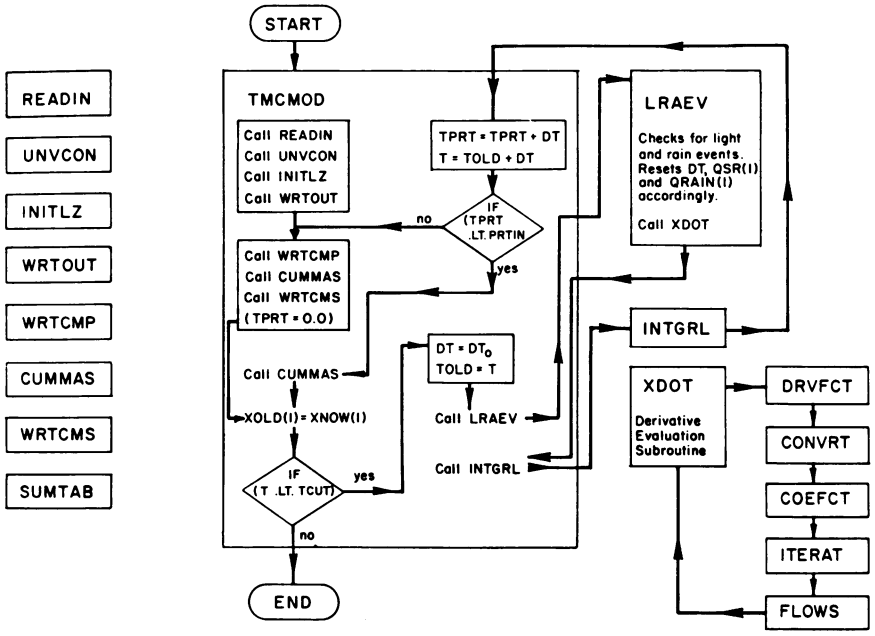

FIGURE 6. Basic NEWTMC flow structure.

requirements are greatly reduced over those that would be required for a program using a finite element or finite difference approximation for the coupled set of nonlinear partial differential equations. Simulations of 40 days using complex soil structures and weather conditions were solved on a VAX/DEC computer.

System Variables

Values for parameters that describe and drive transport of moisture, heat and chemical in unsaturated soils are given in Tables 3–6. The variables that remained constant for the four simulations are listed in Tables 3–5, and those that were varied from run to run are listed in Table 6. Because transport in the soil column is sensitive to the external driving forces occurring in the air chamber, two different rain schedules were used for the 40-day simulations. For both runs, the duration of light and dark, however, were maintained at 14 hr of sunlight followed by 10 hr of darkness. The intensity of sunlight was held constant at 4.16 cal/cm^2-hr, a value corresponding to bright sunlight at 10 A.M., at a latitude of 45°N on June 21 (the latitude of Corvallis, OR). In the first rain schedule, rain accumulation over a period of 10 hr was equal to an inch of rain. In the 40-day time interval, five rain events occurred at a frequency of one every eight days, a rain schedule similar to temperate climates (with this schedule, average annual rainfall is 42 in.). In the second rainfall schedule, rain fell for 2 hr at five different times during a time interval of 40 days, conditions comparable to an extended dry season in a temperate climate. The daylight and darkness schedule and the two rainfall schedules are given in Table 3.

Tables 4 and 5 list values for physical–chemical properties of the air–soil system that were held constant for the four simulation runs. In Table 4, properties that are not varied with depth are listed. Included in this group are basic physical–chemical properties and parameters that describe the moisture tension function and the water conductivity function. In Table 5, properties that are functions of depth are listed. These include layer thickness, porosity, soil constituents, tortuosity, and rate constants for chemical and biological reactions. It should be noted that rate constants for all removal processes are between 10^{-5} and 10^{-6} hr^{-1}, values indicative of nonreactive chemicals.

Table 6 lists variables that are changed from run to run. Variables in this group include dispersivity and adsorptivity coefficients for different soil components. Precise data for these variables were not available, and several values were examined in lieu of either using stochastic methods to select values as a function of

Table 3. Rain schedules for simulations

Day	Time that rainfall started (hours from start)	Time that rainfall stopped (hours from start)
Rainfall for temperate climate: duration of each event was 10 hr at a volumetric flow rate of 2540 cm^3/hr, giving 1.0 in. of rainfall during each interval		
8	194.0	204.0
16	386.0	396.0
24	578.0	588.0
32	770.0	780.0
40	962.0	972.0
Rainfall for extended dry period in a temperate climate: duration of each event was 2 hr at a volumetric flow rate of 1800 cm^3/hr, giving 0.142 in. of rainfall during each interval.		
8	198.0	200.0
16	390.0	392.0
24	582.0	584.0
32	774.0	776.0
40	966.0	968.0

Table 4. Values for variables that remain constant throughout the simulations.

Major region	Symbol	Meaning	Value/units
Soil slab	ρ_{sand}	Density of quartz sand	2.66 g/cm^3
	$\rho_{organic}$	Density of humans	1.30 g/cm^3
	ρ_{clay}	Density of illite clay	2.65 g/cm^3
	α_{soil}	Albedo of soil surface	0.05 (dimensionless)
	α_{water}	Albedo of water surface	0.05 (dimensionless)
	α_{air}	Albedo of water vapor saturated air	0.05 (dimensionless)
	λ_{air}	Conductivity of air at 20°C	0.216 cm-hr-°K
	λ_{water}	Conductivity of water at 20°C	4.932 cal/cm-hr-°K
	λ_{sand}	Conductivity of sand particles	75.6 cal/cm-hr-°K
	$\lambda_{organic}$	Conductivity of organic particles	2.16 cal/cm-hr-°K
	λ_{clay}	Conductivity of clay	25.2 cal/cm-hr-°K
	c_{air}	Specific heat of moist air	0.24 cal/g-°K
	c_w	Specific heat of water	1.0 cal/g-°K
	c_{sand}	Specific heat of quartz sand	0.181 cal/g-°K
	c_{org}	Specific heat of humans	0.46 cal/g-°K
	c_{clay}	Specific heat of illite clay	0.181 cal/g-°K
	ϵH_2O	Emissivity of water	0.95 (dimensionless)
	ϵ_{pexi}	Emissivity of Plexiglass wall	0.95 (dimensionless)
	ϵ_{air}	Emissivity of air above soil	0.90 (dimensionless)
	ϵ_{soil}	Emissivity of soil	0.95 (dimensionless)
	H_c	Henry's law constant	1.73×10^{-7} (dimensionless)
	$D_{l\phi}$	Liquid-phase molecular diffusion coefficient	0.084 cm^2/hr
	$D_{V\phi}$	Vapor-phase molecular diffusion coefficient	252.4 cm$_2$/hr
Soil slab	$\alpha\theta$	Moisture tension function parameter	2.5 cm H_2O
	$\beta\theta$	Moisture function parameter	6.0 (dimensionless)
	$K(\theta)_{sat}$	Saturated moisture conductivity	0.3 cm/hr
	γ_{con}	Moisture conductivity function parameter	7.5 (dimensionless)
Both soil and air chamber	D_{atm}	Water vapor molecular diffusion coefficients in air	0.265 cm^2/sec
	P_{ress}	Air pressure	760.0 mm Hg
	ρ_{air}	Density of air	0.0011 g/cm^3
	ρ_w	Density of water	1.0 g/cm^3
	β_{Tvap}	Temperature effect saturated water vapor density constant	1.05×10^{-6} g/cm^3-°K
	E_{con}	Vaporization of water constant	1.26 cm/hr
	β_{vap}	Vaporization of water due to wind speed constant	1.0 hr/cm
	γ_{Tliq}	Moisture tension temperature effect parameter	-2.09×10^{-3}/°K
	β_{TMC}	Wall reflection factor	0.0
	D_H	Sensible heat transfer variable	1×10^4 cm/hr
	K_{plexi}	Thermal condutivity of TMC Plexiglass wall	0.5 cal/cm-hr-°K
	T_{air}	Outside air temperature	293.0°K
	V_a	Volume of air chamber	10^{12} cm^3
	A	Surface area of afi-soil interface	10^6 cm^2
Both air and soil chambers	q_a	Volumetric airflow rate in air chamber	3×10^{14} cm^3/hr
	q	Gravitational constant	1.2×10^{10} cm/hr^2
	R	Gas constant	5.98×10^{13} cm^2/hr^{2o}-°K
	σ	Stefan-Boltzman constant	4.90×10^{-9} cal/hr-cm^2-°K^{-4}

system variables or approximating these variables with power law functions of moisture content.

Hydraulic conductivity and moisture tension have been represented as power law functions of moisture content. The algorithms of NEWTMC have been constructed to allow the hydraulic conductivity and moisture tension functions to be functions of depth in the soil, making it possible to develop empirical representations for these variables that are sensitive to the characteristics of the soil at that position. The power law representation for moisture tension is given as:

$$\psi(\theta,z) = \alpha_\theta \left\{ 1 - \left[\frac{\theta_{sat}(z)}{\theta(z)} \right]^{\beta\theta} \right\} \qquad (44)$$

where α_θ and β_θ are empirically determined constants; $\theta_{sat}(z)$ is the moisture content at saturation for each soil layer; and $\theta(z)$ is the moisture content of the soil in layer k.

The power law representation for hydraulic conductivity is given as:

$$K(\theta,z) = K(\theta_{sat}) \left[\frac{\theta(z)}{\theta_{sat}(z)} \right]^{\gamma con} \qquad (45)$$

where $K(\theta_{sat})$ is the saturated hydraulic conductivity in the kth soil layer and γ_{con} is an empirically determined constant. Other representations for hydraulic conductivity are given by Gardner (*19*). For the soils presented in the illustrative simulations, a clay silt loam was used

Table 5. Physical–chemical properties of soil layers.

Depth, cm	Porosity (dimensionless)	Tortuosity (dimensionless)	Sand, %	Silt, %	Clay, %	$\beta_l \times 10^6$, hr^{-1}	$\gamma_l \times 10^6$ hr^{-6}	$\alpha_l \times 10^6$ hr^{-1}
1	0.45	0.67	0.40	0.30	0.30	5.0	0.1	4.0
2	0.45	0.67	0.40	0.30	0.30	3.0	0.1	0.8
4	0.45	0.67	0.40	0.30	0.30	1.0	0.1	0.4
7	0.45	0.67	0.35	0.25	0.40	0.8	0.0	0.2
11	0.45	0.66	0.35	0.25	0.40	0.5	0.0	0.1
16	0.45	0.66	0.35	0.25	0.40	0.1	0.0	0.0
26	0.45	0.66	0.35	0.20	0.45	0.0	0.0	0.0
46	0.45	0.65	0.35	0.20	0.45	0.0	0.0	0.0
76	0.45	0.65	0.35	0.20	0.45	0.0	0.0	0.0
126	0.45	0.64	0.35	0.15	0.50	0.0	0.0	0.0
201	0.45	0.63	0.35	0.15	0.50	0.0	0.0	0.0
301	0.45	0.62	0.30	0.15	0.55	0.0	0.0	0.0
401	0.45	0.61	0.30	0.15	0.55	0.0	0.0	0.0
501	0.45	0.60	0.30	0.15	0.55	0.0	0.0	0.0
576	0.45	0.59	0.25	0.15	0.60	0.0	0.0	0.0
626	0.45	0.59	0.25	0.15	0.60	0.0	0.0	0.0
676	0.45	0.58	0.20	0.15	0.65	0.0	0.0	0.0
701	0.45	0.56	0.20	0.10	0.70	0.0	0.0	0.0
711	0.45	0.55	0.20	0.10	0.70	0.0	0.0	0.0
713	0.45	0.55	0.20	0.10	0.70	0.0	0.0	0.0

Table 6. Chemical transport variables.

Run no.	Dispersivity, cm	Adsorption coefficient, cm^3/cm^3 soil water
I. Rainfall for temperate climate		
1	1.0	400.0
2	1.0	4000.0
3	10.0	400.0
4	10.0	4000.0
II. Rainfall for extended dry period		
1A	1.0	400.0
2A	1.0	4000.0
3A	10.0	400.0
4A	10.0	4000.0

(*15*). The length of the soil column was 716 cm; the soil porosity was assumed to be uniform, and the power law constants for the moisture tension and hydraulic conductivity expressions were:

$$\alpha_\theta = 2.5 \text{ cm}; \beta_\theta = 6.0; \gamma_{con} = 6.5; \text{ and } K(\theta_{sat}) = 0.3 \text{ cm/hr} \quad (46)$$

Discussion

In Figures 7 and 8, the hydraulic and chemical responses during single rain events for the two rainfall schedules given in Table 3 and the soil characteristics of Table 5 are shown. In both instances, initially the soils had been allowed to drain to their field capacities.

Figure 7 shows the hydraulic response of the soil column. The responses are similar except in degree of moisture wetting and redistribution with time and position in the soil column. This is due to the amount of water applied to the surface. When the rain stops, the combined effects of evaporation at the surface and gravity drainage quickly drain the water from the top layers of the soil column.

The effects of the amount of rainfall during each event on chemical transport are shown in Figure 8. The mechanisms of many of the processes in the chemical mass balance [Eq. (38)] are not well understood, making it necessary to estimate values for many of the chemical transport variables. Variables that make up this group include reaction rate constants, dispersion coefficients, dispersivities, and adsorption coefficients. The transport of moisture in unsaturated soils, however, has been extensively examined and hydrological data exist for many different soils and for many conditions of saturation and partial saturation (*15–18*). Because the transport of moisture, heat, and chemicals in soils are coupled phenomena and because the transport of moisture is behaving correctly as shown in Figure 7, there is a high probability that the chemical response is also correct.

The intensity and duration of a rainfall event has its most important effect in the upper soil layers. In Figure 8 for the 10-hr rainfall schedule, the concentration varies over a wide range during and after the rain event. There are changes in concentration in the upper soil layers during the 2-hr rainfall schedule, but they are not as extensive. Much of the variation is due to the manner in which concentration is being reported, as micrograms per cubic centimeter of soil water. The more water there is, the greater the dilution. However, at a depth of only several centimeters below the surface, these surface effects damp out quickly, and the responses for both rainfall schedules are similar except penetration is not as great for the soil subjected to the shorter rainfall schedule.

Variations in chemical transport properties and their influence on temporal variations in chemical concentra-

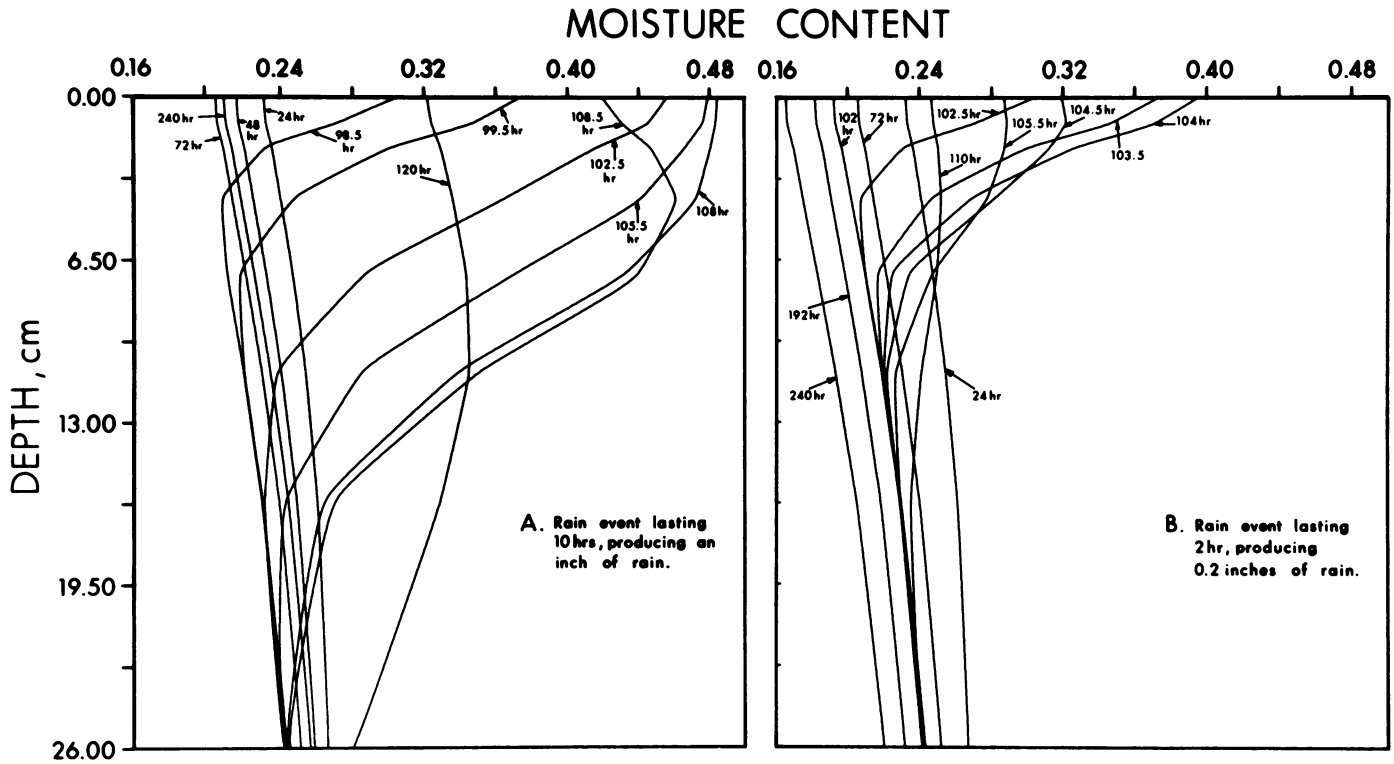

FIGURE 7. Hydrodynamic response of the soil column to (*A*) a 10-hr duration rain event producing 1.0 in. of rain and (*B*) a 2-hr rain event producing 0.2 in. of rain. Soil properties are given in Table 5.

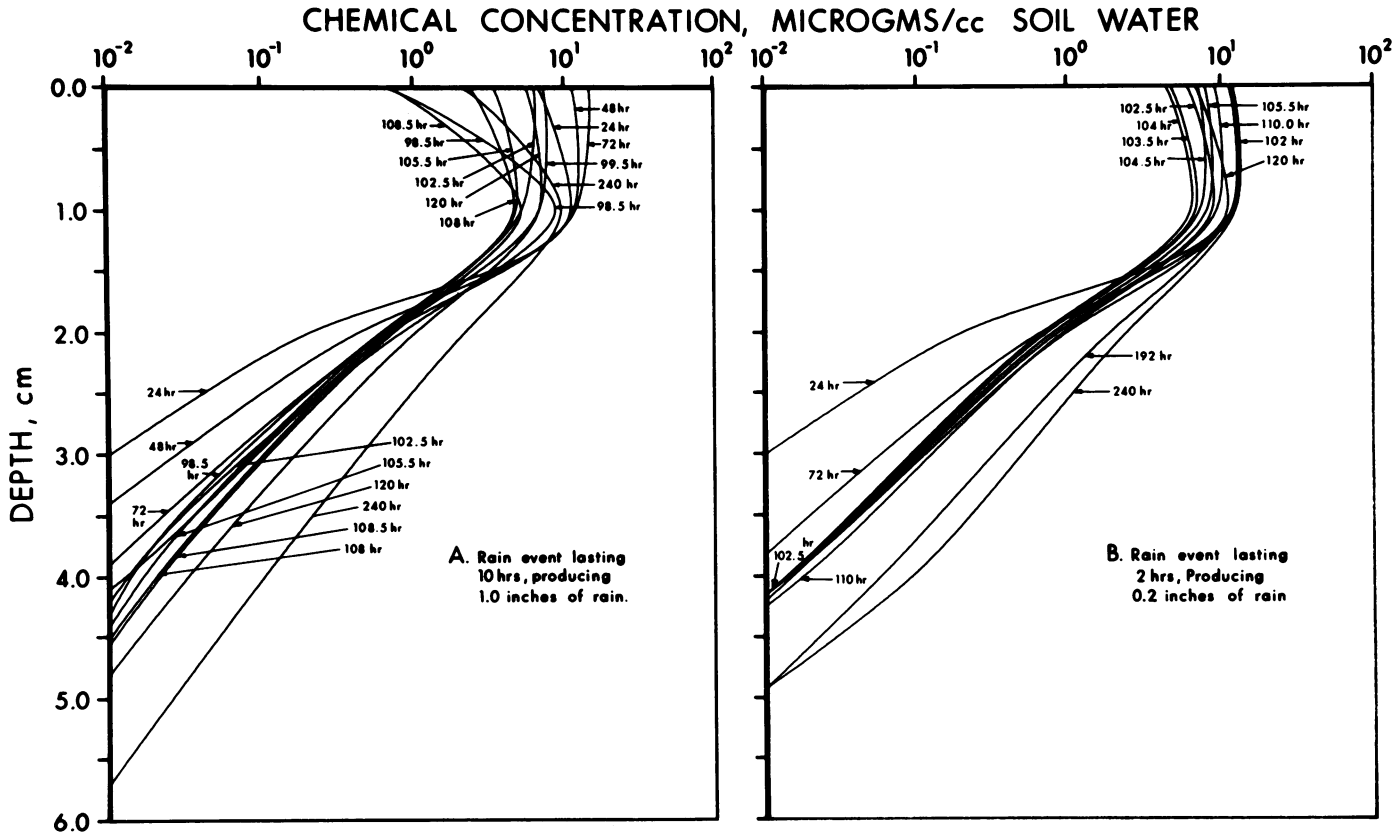

FIGURE 8. Changes in chemical concentration as a function of depth in the soil column for (*A*) the 10-hr rain event producing 1.0 in. of rain, and (*B*) for the 2-hr rain event producing 0.2 in. of rain. Soil properties are given in Table 5; dispersivity = 1.0 cm; adsorption coefficient = 400 cm soil water/cm soil.

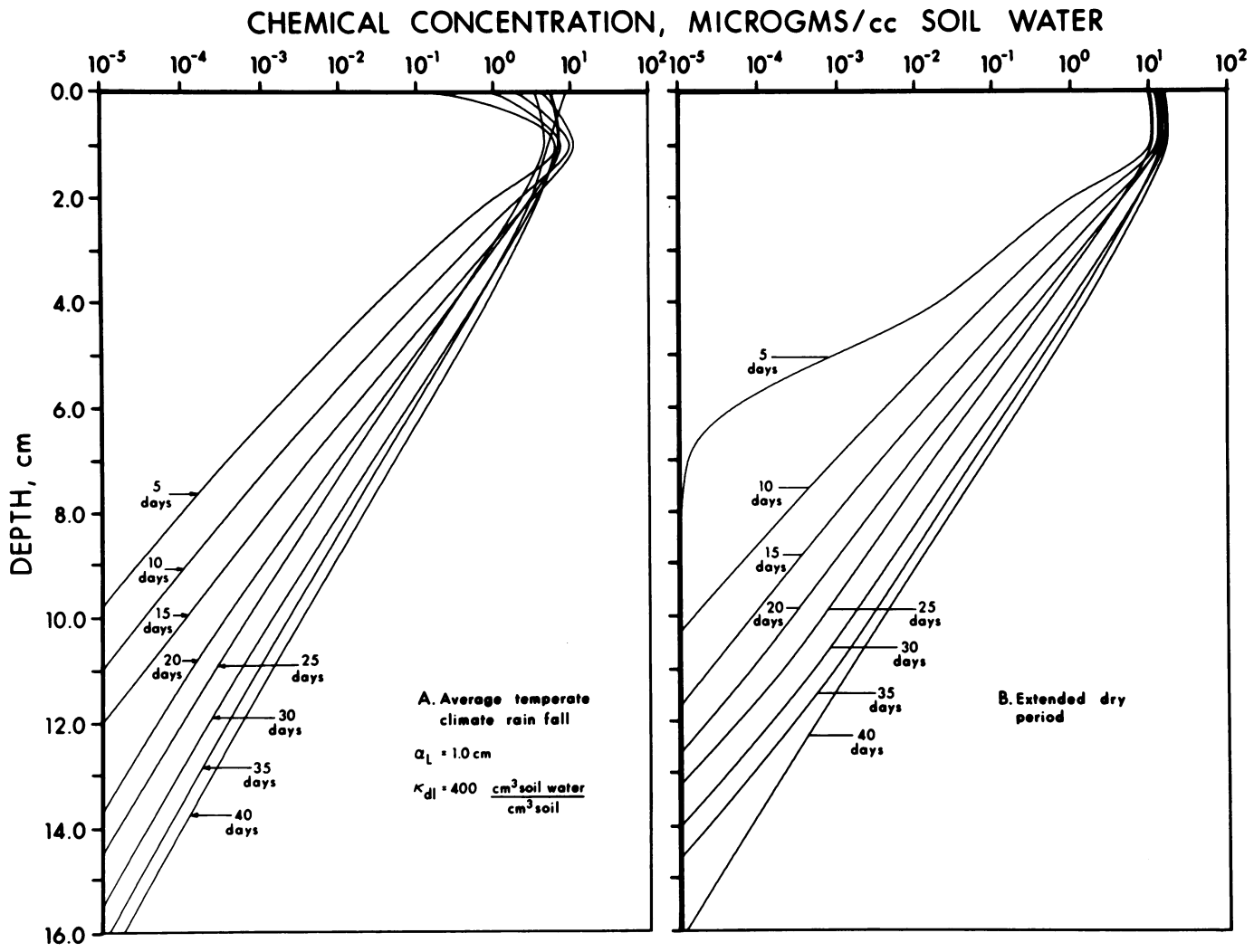

FIGURE 9. Changes in chemical concentration with depth and time for a low water conductivity, low adsorptivity soil and for (*A*) an average temperate climate rainfall schedule and (*B*) for an extended dry period rainfall schedule. Rain schedules are defined in Table 3; soil properties are given in Table 5; dispersivity = 1.0 cm; adsorption coefficient = 400 cm soil water/cm soil.

tion profiles are shown in Figures 9–12. The values for these properties that were changed from run to run are given in Table 6. In each figure, both the heavy and light rainfall schedules are represented, and the chemical concentration profiles are for unreactive chemical substances. The chemical was added to the top soil layer at the start of the simulation.

The effects of these physical–chemical properties on chemical transport are very apparent. When adsorptivities are high and dispersivities low, there is very little movement of the chemical past the top layers of the soil column. On the other hand, for low values of the adsorption coefficient and higher values of the dispersivity coefficient, penetration into the soil column is much greater; however, penetration is still strongly influenced by the amount and frequency of rainfall. Frequency and intensity of rainfall still appears to be the major process that drives the transport of chemical in the soil column.

Because the processes of adsorption and removal of chemicals by biological and chemical means are not well understood, methods of estimating appropriate values for parameters that describe these processes are important topics of investigation. With regard to chemical transport, variations in adsorptivity coefficients for a chemical onto different soil components significantly effect movement of that chemical in unsaturated soils. Other equally unknown mechanisms of actions are removal of chemicals by biological and chemical processes. In the examples presented here, the chemicals were assumed to have a low degree of reactivity both by biological and chemical processes. In addition, it was assumed that the rate of removal could be approximated by first-order reaction-rate kinetics. There is no guarantee that this is an accurate description of these processes. In such a complex structure such as soil, the mechanics of adsorption and reaction on surfaces with variable adsorptivities have not been investigated. To

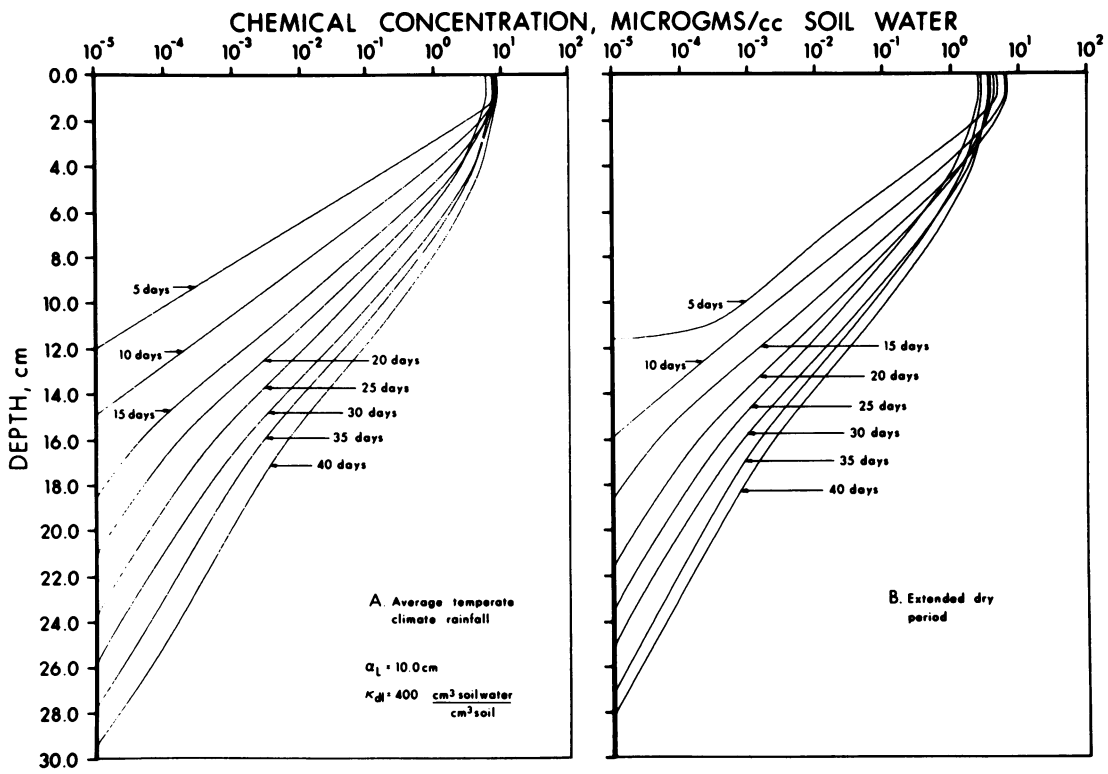

FIGURE 10. Changes in chemical concentration with depth and time for a high water conductivity, low adsorptivity soil and for (*A*) an average temperate climate rainfall schedule and (*B*) for an extended dry period rainfall schedule. Rain schedules are defined in Table 3; soil properties are given in Table 5; dispersivity = 10.0 cm; adsorption coefficient = 400 cm soil water/cm soil.

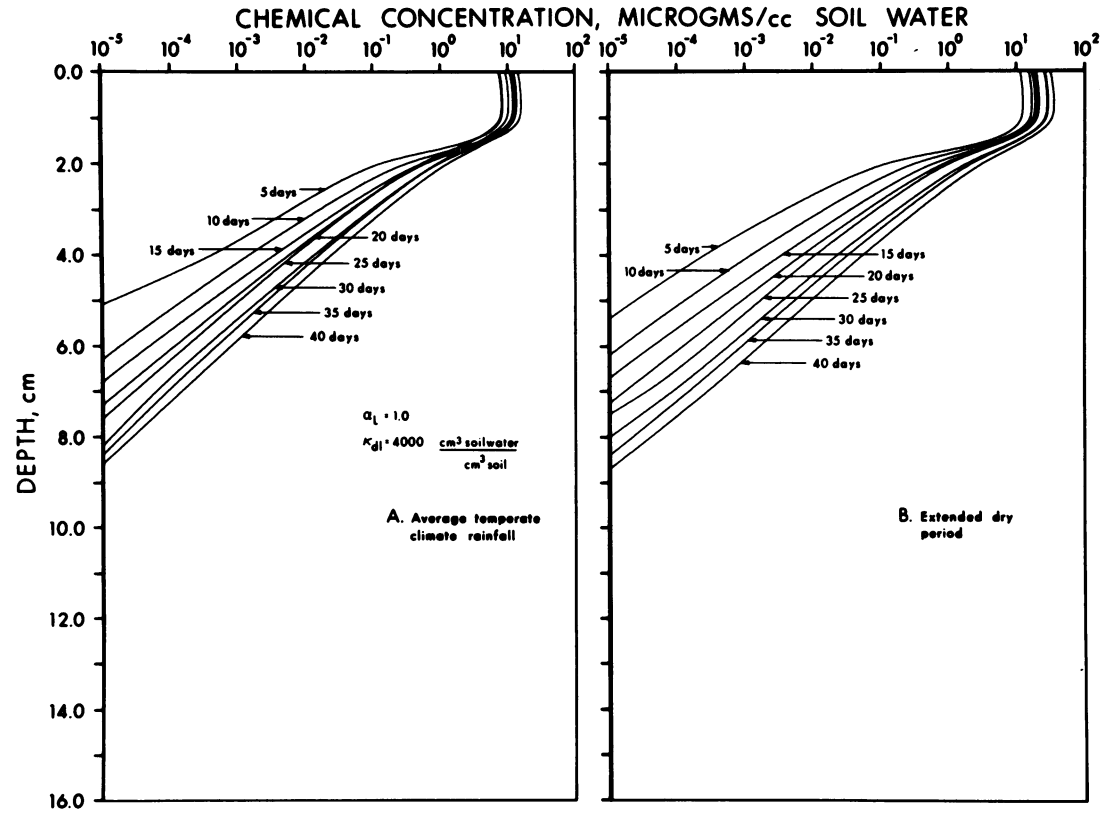

FIGURE 11. Changes in chemical concentration with depths and time for a low water conductivity, high adsorptivity soil and for (*A*) an average temperate climate rainfall schedule and (*B*) for an extended dry period rainfall schedule. Rain schedules are defined in Table 3; soil properties are given in Table 5; dispersivity = 1.0 cm; adsorption coefficient = 4000 cm soil water/cm soil.

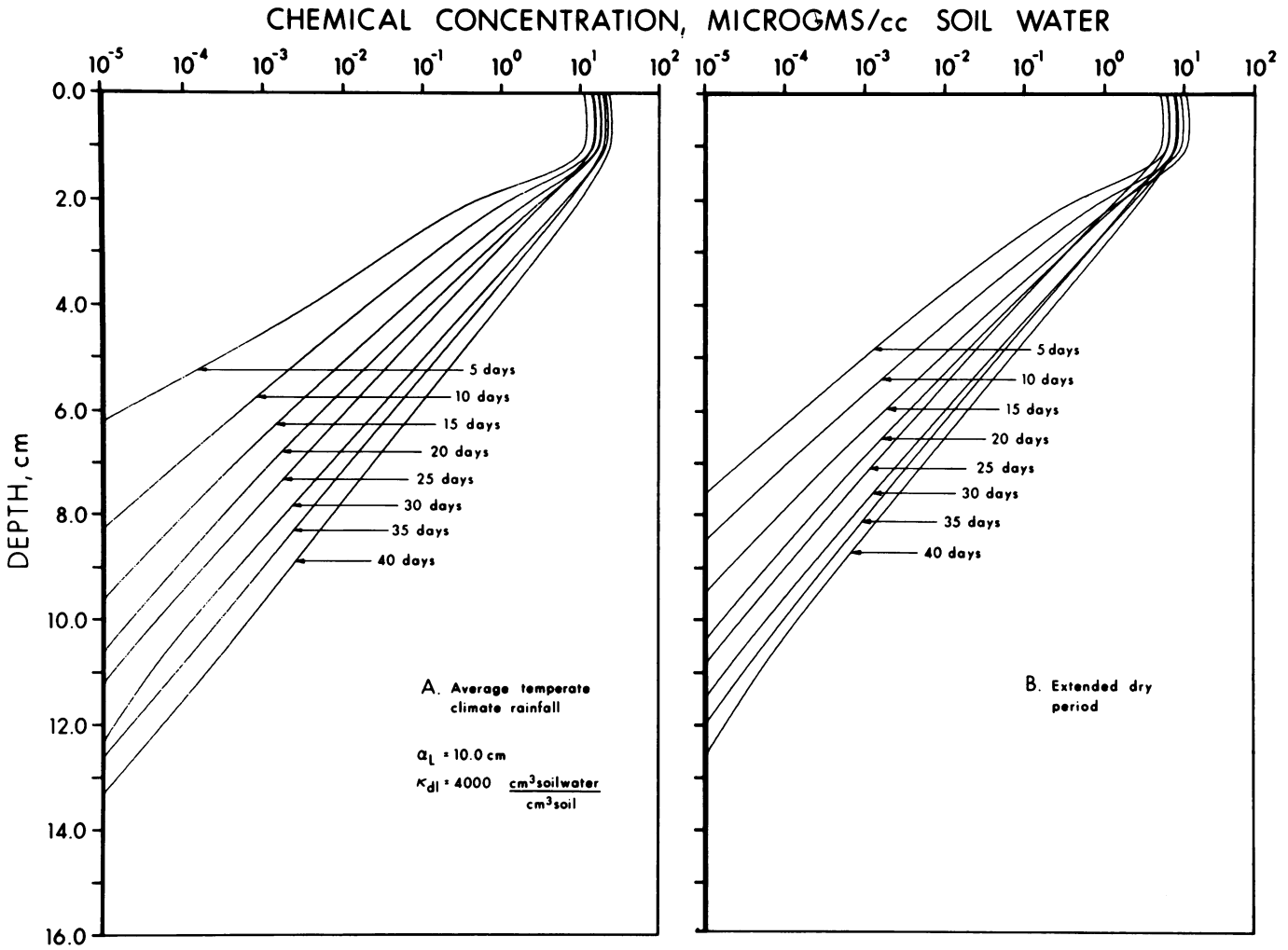

FIGURE 12. Changes in chemical concentration with depth and time for a high water conductivity, high adsorptivity soil for (*A*) an average temperate climate rainfall schedule and (*B*) for an extended dry period rainfall schedule. Rain schedules are defined in Table 3; soil properties are given in Table 5; dispersivity = 10.0 cm; adsorption coefficient = 4000 cm soil water/cm soil.

initiate remedial action for purifying contaminated aquifers, such data are essential.

Degradation of chemicals by microbial metabolism in soils is largely uninvestigated for industrial chemicals. Much attention has been given to the role of microorganisms in nutrient cycling but very little is understood about the ability of microorganisms to metabolize industrial chemicals either as primary or secondary carbon sources. Until recently the unsaturated zone of the soil below the root zone was considered to be biologically dead (*20*). Recent evidence for a limited number of compounds, however, suggests that the number of microorganisms at all depths in the soil does not decline but remains fairly uniform (*21*). The characteristics of these microbial populations, however, are not well understood.

One final note about this model relates to its ability to simulate multicomponent chemical transport. The transport of chemicals from landfills involves the migration of many chemicals. In this situation, terms must be added to account for interactions among the different chemicals and heat and mass transfer equations must be written for each component. In landfills organic solvents can be present resulting in partitioning of chemical components between different liquid phases. Because this situation exists, a single chemical model acting as a surrogate for a mixture of chemicals may only be appropriate when the chemicals are present in low concentrations. If concentrations are low, interactions of all types are usually negligible and the model is a very accurate method for simulating multi-chemical transport in unsaturated soils under a variety of soil conditions and external driving functions.

The initial modeling portions of this research were carried out by F. T. Lindstrom during a six-month IPA with the Corvallis Environmental Research Lab (CERL) division of the U.S. EPA. Initial software development for NEWTMC was supported in part by contract number 808864 for the Toxics and Hazardous Materials Branch, CERL.

REFERENCES

1. Piver, W. T., and Lindstrom, F. T. Waste disposal technologies for polychlorinated biphenyls. Environ. Health Perspect. 59: 163–177 (1985).
2. Lindstrom, F. T., and Piver, W. T. A Mathematical Model for Simulating the Fate of Toxic Chemicals in a Simple Terrestial Microcosm. Technical Report No. 51, Department of Mathematics and Statistics, Oregon State University, Corvallis, OR, 1984.
3. Edlefson, N. E., and Anderson, A. B. C. Thermodynamics of soil moisture. Hilgardia 15: 31–298 (1943).
4. Weast, R. C., and Astle, M. J., Eds. Handbook of Chemistry and Physics, 61st Edition. The Chemical Rubber Company Press Inc., Boca Raton, FL, 1981.
5. Hanks, R. J., and Bowers, S. A. Numerical solution of the moisture flow equation for infiltration into layered soils. Soil Sci. Soc. Amer. Proc. 26: 530–543 91962).
6. Hanks, R. J., Klute, A., and Bresler, E. A numeric method for estimating infiltration, redistribution, drainage, and evaporation of water from soil. Water Resources Res. 5(5): 1064–1069 (1969).
7. Elzy, E., Lindstrom, F. T., Boersma, L., Sweet, R., and Wicks, P. Analysis of the Movement of Hazardous Chemicals in and from a Landfill Site via a Simple Vertical/Horizontal Routing Model. Oregon State University Agricultural Extension Station, Special Report No. 414, Oregon State University, Corvallis, OR, 1974.
8. Price, H. S., Cavendish, J. C., and Varga, R. S. Numerical methods of high order accuracy for diffusion-correction equations. Trans. Soc. Petrol. Engr. J. 243: 293–303 (1968).
9. Reeves, M., and Duguid, J. O. Water Movement through Saturated/Unsaturated Porous Media: A Finite Element Galerkin Model. ORNL Pub. No. 4927, Oak Ridge National Laboratory, Oak Ridge, TN, 1975.
10. Duguid, J. O., and Reeves, M. Material Transport through Porous Media: A Finite Element Galerkin Model. ORNL Pub. No. 4928, Oak Ridge National Laboratory, Oak Ridge, TN, 1976.
11. Milly, P. C. D., and Eagleson, P. S. The Coupled Transport of Water and Heat in a Vertical Soil Column under Atmospheric Excitation. Ralph M. Parsons Lab. Rept. No. 258, MIT, Department of Civil Engineering, Cambridge, MA, 1980.
12. Lapidus, L., and Pinder, G. F. Numerical Solution of Partial Differential Equations in Science and Engineering. Wiley-Interscience, New York, 1982.
13. Milly, P. C. D. Moisture and heat transport in hysteretic, inhomogeneous porous media: a matric head-based formulation and a numerical model. Water Resources Res. 18(3): 489–498 (1982).
14. Philip, J. R. Evaporation, moisture, and heat fields in the soil. J. Meteorol. 14: 359–366 (1957).
15. de Wit, C. T., and Van Keulen, H. Simulation of Transport Processes in Soils. Centre for Agricultural Publishing and Documentation. Waageningen, The Netherlands, 1972.
16. Mualem, Y. Hydraulic conductivity of unsaturated porous media: generalized macroscopic approach. Water Resources Res. 14(2): 325–334 (1978).
17. Segol, G. A three-dimensional Galerkin-finite element model for the analysis of contaminant transport in saturated-unsaturated porous media. In: Finite Elements in Water Resources: Proceedings of the First International Conference on Finite Elements in Water Resources, Princeton University, July 1976 (W. G. Gray, G. F. Pinder and C. A. Brebbia, Eds.), Pentech Press, London, 1977, pp. 2.123–2.144.
18. Warrick, A. W., Biggar, J. W., and Nielsen, D. R. Simultaneous solute and water tranfer for an unsaturated soil. Water Resources Res. 7(5): 1216–1225 (1971).
19. Gardner, W. R. Dynamic aspects of water availability to plants. Soil Sci. 89: 63–73 (1960).
20. Waksman, S. A. Bacteria numbers in soils at different depths, and in different seasons of the year. Soil Sci. 1: 363–380 (1916).
21. Wilson, J. T., Cosby, R. L., and Smith, G. B. Potential for biodegradation of organo-chlorine compounds in ground water. Paper presented at the International Conference on Groundwater Contamination with Organo-Chlorine Compounds of Industrial Origin, Milan, Italy, January 26–29, 1983.